Supplemental Methods

PK/PD/Efficacy Modeling Methodology & PF-2771 Synthetic Methods

A quantitative modeling approach was taken to analyze the relationship between CENP-E inhibitor exposure, intra-tumoral pHH3 response, and tumor growth inhibition in the HCC1806 xenograft mouse model. In the modeling scheme, CENP-E inhibitor exposure (assuming intra-tumoral exposure is approximately in equilibrium with plasma exposure) drives modulation of intra-tumoral pHH3 levels, and in turn modulated pHH3 levels drive inhibition of tumor growth. See **SI Figure S5** for a full model schematic with equations and **Supplementary Tables 4 and 5** for descriptions and values of model parameters and state variables.

PK/PD Analysis

Plasma drug concentrations and tumor levels of phospho-HH3-Ser_{10} in SCID mice bearing orthotopically implanted HCC1806 xenograft tumors (300–500 mm^3) were evaluated for vehicle or a single dose of PF-2771 which was intraperitoneally administered to tumor-bearing mice. Tumors and plasma were collected at 1, 4, 8, 24, or 32 h post-dose (3 mice/time point). For plasma pharmacokinetic experiments, mouse plasma was collected in heparinized vacutainers following intracardiac puncture. The tumor lysates were plated in triplicate on phospho-HH3-Ser_{10} coated ELISA plates (Cell Signaling Technologies) as described by the manufacturer. Plasma concentrations of PF-2771 were measured quantitatively with liquid chromatography–tandem mass spectrometry. The mass spectrometry was performed using electrospray ionization in the positive mode with multiple reaction monitoring (MRM). For analyte, the transition monitored was m/z 554.2 to 155.1, and the declustering potential, collision energy, and exit cell potential were 81, 49, and 16 volts, respectively. For the internal standard, the transition

monitored was m/z 386.3 to 122.2, and the declustering potential, collision energy, and exit cell potential were 81, 43, and 12, respectively. Peak area integration was performed using Analyst 1.4.1 software, and results were electronically exported to Watson 7.4 bioanalytical LIMS (Thermo Scientific, Philadelphia, PA) for curve-fitting and data processing. The calibration curve was run in duplicate and ranged from 1 to 2500 ng/mL.

The plasma free fraction of PF-2771 in SCID mouse plasma was measured using the equilibrium dialysis technique. A total of 3 replicates were prepared for each plasma type and concentration. After incubation, aliquots of plasma (10 μL) and buffer (40 μL) were transferred to separate tubes containing blank buffer (40 μL) and blank plasma (10 μL), respectively, to match matrices. Samples were extracted with 200 μL of acetonitrile containing an internal standard and analyzed by liquid chromatography – tandem mass spectrometry similar to the methods described above. The free fraction in plasma (f_u) was calculated by the equation $f_u = R_{buffer}/R_{plasma}$, where R_{buffer} and R_{plasma} represent the ratio of PF-2771 over internal standard signal intensities in the buffer receiver well and the plasma donor well, respectively.

PK Model

The PK data exhibited a clear biphasic trend when attempting model fitting, resulting in a two-compartment model with linear elimination. A zero-order absorption term was used due to a lack of early time points in the data set, thus not allowing for a robust estimation of a first order absorption rate constant. Volume of distribution was the only parameter found to be significantly dose-dependent. Since the PK model is not intended to be used in a human PK prediction role, no efforts were made to determine the source of the dose dependence.

PD Model

Upon close examination of the intra-tumoral pHH3 data, a clear lag exists between PK C_{max} and peaks in pHH3 modulation, so a standard indirect response model was implemented (with drug effect inhibiting dephosphorylation of pHH3). However, the lag in effect from drug exposure was significant enough not to allow for good model fits to data using the standard indirect response model. Therefore, a transit compartment model was implemented (see **SI Figure 5**) that accounts for significant lag in effect, similar to the model presented in Krzyzanski, *et al.* (1999). Furthermore, we found that the relationship between drug exposure and pHH3 response is nonlinear, so a Hill function was implemented to characterize the modulation of pHH3. As seen in **SI Figure S4**, this model structure adequately captured the time course of pHH3 modulation.

In the estimation process, parameter correlation issues arose with the maximum effect parameter, E_{max}, and the Hill coefficient. Based on observed model behavior relative to the data, these values were both set to 1. In short, setting the Hill coefficient to anything significantly above 1 resulted in much poorer fits to the data. Setting $E_{max} = 1$ physiologically means that the CENP-E inhibitor can theoretically inhibit dephosphorylation of pHH3 100%. This assumption is physiologically plausible, and we know of no data to suggest the contrary. Therefore, both of these assumptions remained in the model throughout fitting and simulations.

TGI Model

The PD model described above was used to drive tumor growth inhibtion in the TGI model. Examining the growth curves in the control group (see **SI Figure S4**), one can easily see that

growth slows significantly once the tumors reach a certain size. Therefore, we implemented a logistic-growth model similar to what is presented in Yang, *et al.* (2010), where the transit compartments are collapsed to a single compartment. In the model, each animal was assigned its own initial tumor volume, based on data. This results in multiple simulation curves for each dose group in the TGI plots in **SI Figure S4**.

We refer the reader to the main text, where we describe the lack of a robust exposure-biomarker response-TGI relationship within the dose range of the studies conducted. This resulted in the choice of a linear term in the model for pHH3-driven effects on tumor growth (see the equations in **SI Figure 5**). With a more comprehensive exposure-biomarker response-TGI data set, the assumption of linearity may not hold, and a nonlinear term would need to be considered. However, with the current data set, the linear term allowed the model to adequately capture the dynamics of the TGI (see **SI Figure S4**).

SI Figure S5. PK/PD/TGI model schematic and equations. The schematic depicts the model in a set of coupled modules, labeled *PK*, *PD* and *TGI*. The final panel contains the equations for the model. The model's state variables and parameters are defined in **SI Tables S4 and S5**. The highlighted terms in the equations labeled "Grow" and "Kill" correspond to the aforesaid labels appearing in the *TGI* module.

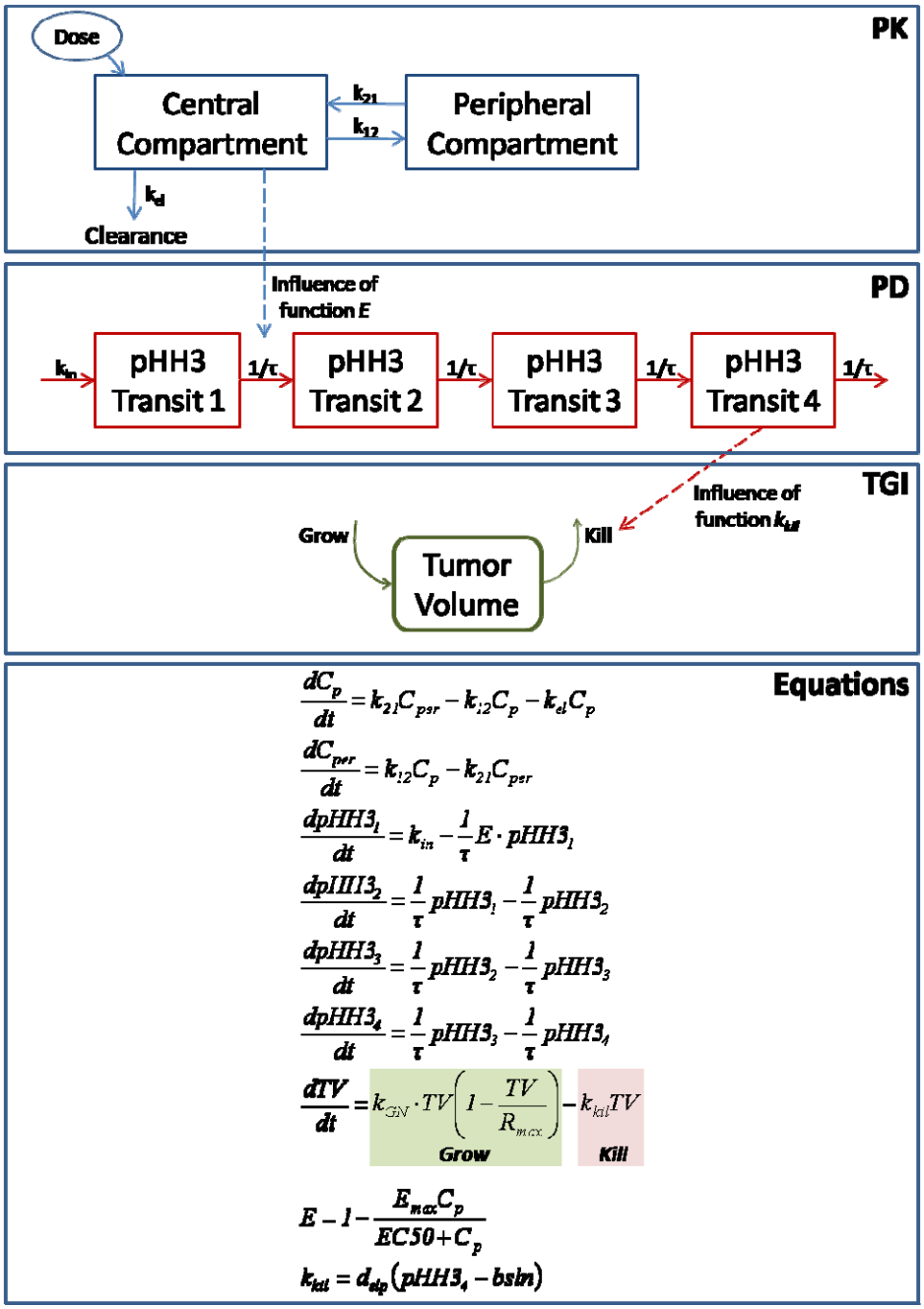

PK/PD/TGI model schematic and equations. The schematic depicts the model in a set of coupled modules, labeled *PK*, *PD* and *TGI*. The final panel contains the equations for the model. The model's state variables and parameters are defined in **SI Tables S4 and S5**. The highlighted terms in the equations labeled "Grow" and "Kill" correspond to the aforesaid labels appearing in the *TGI* module.

SI Table S4. PK model parameters and state variables.

	Name	Description	Value			
Variable	C_p	Drug concentration in central (plasma) compartment	0*			
	C_{per}	Drug concentration in peripheral compartment	0*			
			Dose (mg/kg)			
			3	*10*	*30*	*100*
Parameter	CL**	Central compartment clearance (L/hr)	3.06	3.57	3.05	1.36
	$V1$	Apparent volume of central compartment (L)	4.14	7.02	5.12	3.76
	$V2$	Apparent volume of peripheral compartment (L)	21.68	21.17	10.58	2.43
	Q	Inter-compartment flux (1/hr)	0.757	0.757	0.757	0.757

*Initial values at beginning of simulation
**In the model, $k_{el} = CL/V1$

SI Table S5. PD/TGI model parameters and state variables.

	Name	Description	Value
Variable	$pHH3_1$	pHH3 transit compartment	$bsln$*
	$pHH3_2$	pHH3 transit compartment	$bsln$*
	$pHH3_3$	pHH3 transit compartment	$bsln$*
	$pHH3_4$	pHH3 transit compartment	$bsln$*
	TV	Tumor volume (mm^3)	Varies*,**
Parameter	k_{in}	Rate of HH3 phosphorylation	$bsln$*$1/\tau$***
	$1/\tau^{est}$	Transit rate constant (1/hr)	1.12
	k_{GN}^{est}	Tumor growth rate constant (1/hr)	0.0156
	R_{max}^{est}	Logistic maximum tumor volume (mm^3)	1160
	E_{max}	Maximum drug effect on pHH3	1
	$EC50^{est}$	Drug concentration at 50% maximum effect (ng/mL)	102****
	d_{slp}^{est}	Linear slope for pHH3 effect on TGI	0.008
	$bsln^{est}$	pHH3 level at steady state	0.318

*Initial values at beginning of simulation
**Each individual animal started in the simulations with its own initial tumor volume, and the value used is the initial volume reported from the data set
***To force pHH3 steady state in unperturbed state
****102 ng/mL total (plasma) = 4.07 nM free (plasma)
estParameter is estimated from data

PK/PD References

Krzyzanski W, Ramakrishnan R, Jusko WJ. Basic pharmacodynamic models for agents that alter production of natural cells. *J Pharmacokinet Biopharm.* 1999 Oct; 27(5):467-89

Yang J, Mager DE, Straubinger RM. Comparison of two pharmacodynamic transduction models for the analysis of tumor therapeutic responses in model systems. *AAPS J.* 2010 Mar; 12(1):1-10

Supplementary Materials and Methods

Synthesis of the CENP-E inhibitor PF-2771

SI Scheme S1. Synthetic scheme of PF-2771.

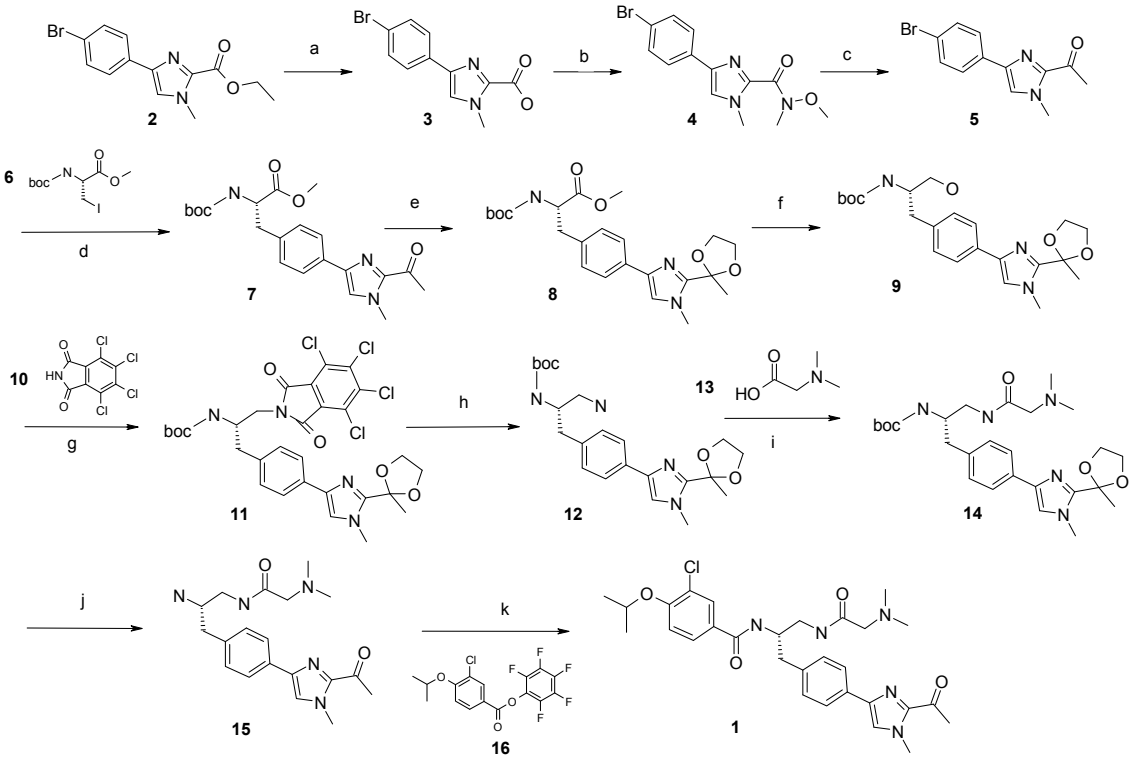

Conditions: a) NaOH, MeOH, rt, O.N., quant. yield; b) HATU, TEA, 60°C, 3 h, 67%; c) MeMgBr, 0°C, 30 min, 92%; d) 1. **6**, Zn, $BrCH_2CH_2Br$, TMSCl; 2. $Pd_2(dba)_3$/P(o-Tol)$_3$, DMF, 60°C, 2 h, 88%; e) glycol/THF, TsOH, reflux, O.N., 62%; f) $NaBH_4$, MeOH, 65°C, 2 h; g) **10**, DIAD, Ph_3P, THF, rt, O.N., 32%, two steps; h) NH_2NH_2, MeOH, rt, O.N.; i) **13**, HATU, TEA, 60°C, 5 h, 62%, two steps; j) 6M HCl, THF/H_2O, reflux, O.N.;k) **16**, TEA, DMF, rt, 3 h, 61%, two steps.

4-(4-bromophenyl)-1-methyl-1*H*-imidazole-2-carboxylic acid (**3**):

A mixture of **2** (2.0 g, 6.47 mmol), NaOH (9.7 mL, 19.4 mmol, 2 N NaOH aqueous solution), and 20 mL MeOH was stirred at rt for O.N. After removing volatiles, the resulting residue was diluted with water (50 mL), and neutralized to pH = ~ 3 with 1 M HCl (~20 mL), and diluted with a small amount of MeCN, chilled in acetone/dry ice bath, and lyophilized to afford the title compound as a solid with 3 eq NaCl (2.95 g, quant. yield). LCMS: (M-CO_2) = 237.20.

4-(4-bromophenyl)-*N*-methoxy-*N*,1-dimethyl-1*H*-imidazole-2-carboxamide (**4**):

To a reaction vessel were charged **3** (1.82 g, 6.47 mmol), O,N-Dimethyl-hydroxylamine HCl (947 mg, 9.71 mmol), HATU (2.71 g, 7.12 mmol), TEA (2.71 mL, 19.4 mmol, neat), and 30 mL anhydrous DMF. The resulting reaction was heated at 60°C for 3 h. After cooling down to rt, the reaction mixture was partitioned between water (150 mL) and ethyl acetate (200 mL). The organic phase was separated, washed with sat. sodium bicarbonate (1x150mL), brine (2 x 150 mL), dried over sodium sulfate, and concentrated to dryness. The resulting crude material was purified by column with a gradient elution of 50% EA/HEP→EA to afford the title compound as a solid (1.4 g, 67% yield over two steps). 1H NMR (400 MHz, DMSO-d6) δ ppm: 7.89 (s, 1 H), 7.72 (d, J = 8.6 Hz, 2 H), 7.57 (d, J = 8.3 Hz, 2 H), 3.82 (s, 3 H), 3.80 (s, 3 H), 3.43 (br. s., 3 H). LCMS: (M+H) = 324.20.

1-[4-(4-bromophenyl)-1-methyl-1*H*-imidazol-2-yl]ethanone (**5**):

A solution of **4** (1.34 g, 4.13 mmol) in 30 mL anhydrous THF was cooled to 0°C, and treated with methyl magnesium bromide (4.13 mL, 1.24 mmol, 3 M in ether) under nitrogen. The resulting reaction mixture was maintained at 0°C for 30 min, quenched into water (2 mL), diluted with sat. sodium bicarbonate (50 mL), extracted with ether (2x100mL). The organic phase was dried over anhydrous sodium sulfate, concentrated in vacuo to dryness, and purified by column with a gradient elution of 20→60% EA/HEP to afford the title compound as a solid (1.06 g, 92% yield). 1H NMR (400 MHz, *DMSO-d6*) δ ppm: 8.04 (s, 1 H), 7.77 (d, J = 8.3 Hz, 2 H), 7.60 (d, J = 8.6 Hz, 2 H), 3.94 (s, 3 H), 2.59 (s, 3 H). LCMS: (M+H) = 279.00.

methyl 4-(2-acetyl-1-methyl-1*H*-imidazol-4-yl)-*N*-(*tert*-butoxycarbonyl)-L-phenylalaninate (**7**):

To a suspension of zinc dust (2.81 g, 43.0 mmol, <10μm) in dry degassed DMF (20 mL) was added 1,2-dibromoethane (124 μL, 1.43 mmol) under nitrogen. The mixture was heated with a heat gun for about 30 sec until gas started to evolve from the solution, indicating the activation of

zinc.The mixture was allowed to cool to rt, followed by the addition of TMS-Cl (182 μL, 1.43 mmol), and allowed to stir at rt for 30 min. A solution of **6** (2.59 g, 7.88 mmol) in dry degassed DMF (10 mL) was added to the zinc solution, and the resulting mixture was stirred at rt for 1 h. After allowing zinc to settle, the reaction mixture was filtered through a syringe filter into a mixture of **5** (2.0 g, 7.16 mmol) in dry degassed DMF (10 mL), $Pd_2(dba)_3$ (328 mg, 0.358 mmol), and tri-o-tolyphosphine (436 mg, 1.43 mmol). The reaction mixture was flushed with nitrogen, and stirred at 60°C for 2 h. After cooling down to rt, the reaction mixture was partitioned between water (150 mL) and ethyl acetate (200 mL). The organic phase was separated, washed with brine (2 x 150 mL), dried over sodium sulfate, concentrated to dryness, and purified by column with a gradient elution of 50% EA/HEP→ EA to afford the title compound as a foam (2.52 g, 88% yield). 1H NMR (400 MHz, chloroform-*d*) δ ppm: 7.74 (d, J = 7.8 Hz, 2 H), 7.29 (s, 1 H), 7.18 (d, J = 8.1 Hz, 2 H), 5.00 (d, J = 7.3 Hz, 1 H), 4.52 - 4.69 (m, 1 H), 4.04 (s, 3 H), 3.74 (s, 3 H), 3.04 - 3.22 (m, 2 H), 2.73 (s, 3 H), 1.45 (s, 9 H). LCMS: (M+H) = 402.20.

methyl *N*-(*tert*-butoxycarbonyl)-4-[1-methyl-2-(2-methyl-1,3-dioxolan-2-yl)-1*H*-imidazol-4-yl]-L-phenylalaninate (**8**):

A mixture of **7** (900 mg, 2.24 mmol), p-toluenesulfonic acid monohydrate (96 mg, 0.505 mmol), trimethyl orthoformate (7.5 mL, 68.6 mmol) in 10 mL ethylene glycol, and 10 mL THF was refluxed for O.N. LCMS showed that the reaction was about 50% complete. More p-toluenesulfonic acid monohydrate was added until the reaction almost to be completed. After cooling down to rt, the reaction mixture was diluted with 100 mL ethyl acetate, and washed with 2 M Na_2CO_3 (1x100mL), water (2x100mL), brine (1x100mL), dried over sodium sulfate, concentrated to dryness, and purified by column with a gradient elution of 50% EA/HEP→ EA

to afford the title compound as an oil (619 mg, 62% yield). 1H NMR (400 MHz, *CHLOROFORM-d*) δ ppm: 7.69 (δ, J = 8.1 Hz, 2 H), 7.03 - 7.16 (m, 3 H), 4.95 (d, J = 8.1 Hz, 1 H), 4.49 - 4.63 (m, 1 H), 4.08 - 4.18 (m, 2 H), 3.93 - 4.06 (m, 2 H), 3.78 (s, 3 H), 3.70 (s, 3 H), 2.98 - 3.15 (m, 2 H), 1.81 (s, 3 H), 1.43 (s, 9 H). LCMS: (M+H) = 446.20.

tert-butyl [(2*S*)-1-hydroxy-3-(4-[1-methyl-2-(2-methyl-1,3-dioxolan-2-yl)-1*H*-imidazol-4-yl]phenyl)propan-2-yl]carbamate (**9**):

A suspension of **8** (575 mg, 1.29 mmol) and $NaBH_4$ (293 mg, 7.75 mmol) in 10 mL anhydrous THF was stirred at 65^{o}C for 15 min. Methanol (10 mL) was then added dropwise. Lots of bubbles were generated. The resulting reaction was stirred at 65^{o}C for additional 1 h. After cooling down to rt, the reaction mixture was poured into 2 M ammonium chloride (50 mL), and stirred for another 30 min, and extracted with ethyl acetate (3x50mL). The combined organic phase was dried over sodium sulfate, and concentrated to afford the title compound without further purification. LCMS: (M+H) = 418.20/419.20.

tert-butyl [(2*S*)-1-(4-[1-methyl-2-(2-methyl-1,3-dioxolan-2-yl)-1*H*-imidazol-4-yl]phenyl)-3-(4,5,6,7-tetrachloro-1,3-dioxo-1,3-dihydro-2*H*-isoindol-2-yl)propan-2-yl]carbamate (**11**):

Under a nitrogen atmosphere, DIAD (242 mg, 1.94 mmol) in 4 mL anhydrous THF was added dropwise at 0°C to a solution of triphenyl phosphine (508 mg, 1.94 mmol) in 20 mL anhydrous THF, followed subsequently by adding **10** (441 mg, 1.55 mmol), and **9** (539 mg, 1.29 mmol) in 4 mL anhydrous THF. The resulting reaction mixture was allowed to warm to rt, and stir at 60°C for O.N. After cooling down to rt, the reaction mixture was concentrated to dryness, and purified by column with a gradient elution of 20%EA/HEP→ EA to afford the title

compound as a solid (281 mg, 32%, two steps). 1H NMR (400 MHz, *CHLOROFORM-d*) δ ppm: 7.66 (d, J = 7.07 Hz, 2 H), 7.17 (d, J = 7.6 Hz, 2 H), 7.03 (s, 1 H), 4.57 (d, J = 7.8 Hz, 1 H), 4.26 - 4.44 (m, 1 H), 4.09 - 4.20 (m, 2 H), 3.96 - 4.08 (m, 2 H), 3.78 (s, 3 H), 3.68 - 3.76 (m, 2 H), 2.95 (dd, J = 14.0, 5.9 Hz, 1 H), 2.80 (dd, J = 14.0, 7.5 Hz, 1 H), 1.82 (s, 3 H), 1.30 (s, 9 H). LCMS: (M+H) = 683.00.

tert-Butyl [(2*S*)-1-amino-3-(4-[1-methyl-2-(2-methyl-1,3-dioxolan-2-yl)-1*H*-imidazol-4-yl]phenyl)propan-2-yl]carbamate (**12**):

To a solution of **11** (265 mg, 0.387 mmol) in 8 mL MeOH was added hydrazine 1-hydrate (0.2 mL, 4.04 mmol). After stirring at rt for O.N., precipitates were formed, filtered, washed with ethyl acetate. The organic phase was concentrated to afford the desired product without further purification. LCMS: (M+H) = 417.20.

tert-butyl [(2*S*)-1-[(*N*,*N*-dimethylglycyl)amino]-3-(4-[1-methyl-2-(2-methyl-1,3-dioxolan-2-yl)-1*H*-imidazol-4-yl]phenyl)propan-2-yl]carbamate (**14**):

A solution **12** (161 mg, 0.387 mmol, crude) in 2 mL anhydrous DMF was added into a solution of **13** (120 mg, 1.16 mmol), HATU (441 mg, 1.16 mmol), and TEA (0.27 mL, 1.94 mmol, neat) in 4 mL anhydrous DMF. The resulting reaction mixture was heated at 60°C for 3 h. After cooling down to rt, the reaction mixture was diluted with 50 mL ethyl acetate, washed with saturated sodium bicarbonate (2 x 50 mL), brine (1 x 50 mL), dried over sodium sulfate, concentrated to dryness, and purified by column with a gradient elution of EA→10% MeOH/EA to afford the title compound as a solid (121 mg, 62% yield, two steps). 1H NMR (400 MHz, *CHLOROFORM-d*) d ppm: 7.71 (d, J = 7.6 Hz, 2 H), 7.39 (br. s., 1 H), 7.19 (d, J = 7.3 Hz, 2 H),

7.09 (s, 1 H), 4.97 (br. s., 1 H), 4.09 - 4.26 (m, 2 H), 3.99 - 4.09 (m, 2 H), 3.86 - 3.99 (m, 1 H), 3.79 (s, 3 H), 3.19 - 3.43 (m, 2 H), 2.95 (s, 3 H), 2.62 - 2.79 (m, 1 H), 2.28 (s, 6 H), 1.82 (s, 3 H), 1.43 (s, 9 H). LCMS: (M+H) = 502.20.

N-((2*S*)-3-[4-(2-acetyl-1-methyl-1*H*-imidazol-4-yl)phenyl]-2-aminopropyl)-N^2,N^2-dimethylglycinamide (**15**):

To a solution of **14** (121 mg, 0.241 mmol) in 10 mL anhydrous THF was added dropwise 6 M HCl (1.0 mL, 6.0 mmol). The resulting reaction mixture was stirred at 60 °C for O.N. LCMS: (M+H) = 358.20. Concentrating to dryness afforded the title compound without further purification for next step.

N-((2*S*)-1-[4-(2-acetyl-1-methyl-1*H*-imidazol-4-yl)phenyl]-3-[(*N*,*N*-dimethylglycyl)amino]propan-2-yl)-3-chloro-4-(propan-2-yloxy)benzamide (**1,** PF-2771):

A mixture of **15** (121 mg, 0.24 mmol), **16** (136 mg, 0.357 mmol), and TEA (0.5 mL, 3.59 mmol) in 8 mL anhydrous DMF was stirred at rt for 3 h. The reaction mixture was diluted with ethyl acetate (50mL), washed with water (1 x50 mL), saturated sodium bicarbonate (1 x 50 mL), brine (1 x 50 mL), dried over sodium sulfate, concentrated to dryness, and purified by column with a gradient elution of EA →10% MeOH/EA to afford the title compound as a solid (81 mg, 61% yield over two steps). 1H NMR (400 MHz, *CHLOROFORM-d*) δ ppm: 7.93 (d, J = 2.0 Hz, 1 H), 7.76 (d, J = 8.1 Hz, 2 H), 7.66 (dd, J=8.6, 2.0 Hz, 1 H), 7.50 - 7.63 (m, 2 H), 7.29 - 7.36 (m, 3 H), 6.96 (d, J = 8.6 Hz, 1 H), 4.55 - 4.70 (m, 1 H), 4.30 - 4.45 (m, 1 H), 4.05 (s, 3 H), 3.45 - 3.57 (m, 1 H), 3.19 - 3.38 (m, 2 H), 2.88 - 3.04 (m, 2 H), 2.65 - 2.82 (m, 4 H), 2.28 (s, 6 H), 1.41 (d, J = 6.1 Hz, 6 H). LCMS: (M+H) = 554.20.